Applied Microbiology and Biotechnology (2024) 108:460
https://doi.org/10.1007/s00253-024-13291-3

BIOTECHNOLOGICALLY RELEVANT ENZYMES AND PROTEINS

# Enhancing catalytic efficiency of *Bacillus subtilis* laccase BsCotA through active site pocket design

**Yiqia Hou[1] · Lijun Zhao[1] · Chen Yue[1] · Jiangke Yang[1] · Yanli Zheng[1] · Wenfang Peng[2] · Lei Lei[1]**

Received: 22 February 2024 / Revised: 19 August 2024 / Accepted: 21 August 2024 / Published online: 5 September 2024


## Abstract

BsCotA laccase is a promising candidate for industrial application due to its excellent thermal stability. In this research, our objective was to enhance the catalytic efficiency of BsCotA by modifying the active site pocket. We utilized a strategy combining the diversity design of the active site pocket with molecular docking screening, which resulted in selecting five variants for characterization. All five variants proved functional, with four demonstrating improved turnover rates. The most effective variants exhibited a remarkable 7.7-fold increase in catalytic efficiency, evolved from $1.54 \times 10^5$ $M^{-1}$ $s^{-1}$ to $1.18 \times 10^6$ $M^{-1}$ $s^{-1}$, without any stability loss. To investigate the underlying molecular mechanisms, we conducted a comprehensive structural analysis of our variants. The analysis suggested that substituting Leu386 with aromatic residues could enhance BsCotA's ability to accommodate the 2,2′-azino-di-(3-ethylbenzothiazoline)-6-sulfonate (ABTS) substrate. However, the inclusion of charged residues, G323D and G417H, into the active site pocket reduced $k_{cat}$. Ultimately, our research contributes to a deeper understanding of the role played by residues in the laccases' active site pocket, while successfully demonstrating a method to lift the catalytic efficiency of BsCotA.

### Key points

- *Active site pocket design that enhanced BsCotA laccase efficiency*
- *7.7-fold improved in catalytic rate*
- *All tested variants retain thermal stability*

**Keywords** CotA laccase · Active site design · Laccase engineering · Rational design · Substrate specificity

## Introduction

Laccases are a class of copper-containing oxidases that facilitate the oxidation of a broad range of phenolic compounds (Hakulinen and Rouvinen 2015). Unlike other oxidases, laccases directly utilize dioxygen as the electron acceptors and yield only water as a byproduct, forgoing the production of hydrogen peroxide, radical compounds, or other oxidants (Mate and Alcalde 2017; Morozova et al. 2007). Due to their capacity to degrade diverse pollutants in an eco-friendly way, laccases have drawn considerable interest in fields like toxic wastewater treatment, dye decolorization, and pulp bleaching (Mate and Alcalde 2015; Shankar and Shikha 2014). Moreover, laccases have been harnessed as biocatalysts in several chemical synthesis studies (Riva 2006). The *Bacillus subtilis* spore-associate protein CotA, one of the most frequently studied bacterial laccases (Martins et al. 2002), exhibits high-temperature resistance and alkaline tolerance (Henriques and Moran 2007; Klobutcher et al. 2006). Capable of catalyzing a wide array of substrates (Reiss et al. 2011), BsCotA has demonstrated significant potential for multiple applications such as biochemical pulping for lignin degradation (Ihssen et al. 2017), textile dyes' decolorization (Reiss et al. 2011), and aflatoxin $B_1$ detoxification (Guo et al. 2020).

In most practical applications of laccases, mediators are necessary (Vetting et al. 2015). These mediators also serve as substrates for laccases, functioning as electron shuttles to facilitate the oxidation of stubborn

✉ Lei Lei
lei_bc@whpu.edu.cn

[1] School of Life Science and Technology, Wuhan Polytechnic University, Wuhan 430023, People's Republic of China

[2] State Key Laboratory of Biocatalysis and Enzyme Engineering, College of Life Science, Hubei University, Wuhan 430062, People's Republic of China

compounds (Camarero et al. 2002). ABTS (2,2′-azino-di-(3-ethylbenzothiazoline)-6-sulfonate) is one of the most frequently employed mediators in laccase applications (Gupta et al. 2010). From an industrial standpoint, amplifying the performance of laccases against the mediator ABTS could lower both the amount of mediator required and the incubation period, thereby cutting costs and boosting productivity.

Here, in this study, we endeavored to improve the ABTS oxidation activity of BsCotA laccase by modifying the active site pocket. Drawing on the published BsCotA structure (PDB id: 3ZDW) (Enguita et al. 2004), we pin-pointed 8 residues, within a 4 Å radius of the ABTS molecule, that might involve in the interactions between BsCotA and the ABTS ligand. Utilizing the FuncLib algorithm (Khersonsky et al. 2018), we devised a collection of multi-point mutations focusing stability and functional versatility. Subsequently, we performed molecule docking to identify the variants potentially exhibiting higher catalytic efficiency, utilizing RosettaLigandDocking (DeLuca et al. 2015; Nguyen et al. 2013). The five variants with the finest virtual screening scores were synthesized, expressed, purified, and characterized. All variants demonstrated an enhanced $k_{cat}/K_M$, with the F-09 variant showing a reduced $K_M$ and an improved $k_{cat}$, constituting an approximately ~ 7.7-fold improvement in $k_{cat}/K_M$ compared to the wild-type.

## Materials and methods

### Substrate docking of ABTS with BsCotA laccase (PDB: 3ZDW)

The conformers of ABTS were generated using the BCL::ConformerGeneration program (Kothiwale et al. 2015). The RosettaLigand in Rosetta3.11 (DeLuca et al. 2015) was employed for docking ABTS molecule into the BsCotA protein structure. The docking process involved two steps: (1) a low-resolution docking, which allowed the ligand to explore the space within 7.0 Å of the T1 copper ion while keeping the protein rigid, and (2) a high-resolution docking step, that combined protein side-chain rotamer and ligand conform sampling to optimize the protein-ABTS complex conformation.

We carried out docking for 50 variants along with the wild-type. For each variant, we generated 2000 simulated protein-ABTS complexes and calculated the interface scores using the REF2015 score function (O'Meara et al. 2015). We selected the complex with the best ligand interface score to represent the catalytic efficiency of the BsCotA variant for ABTS.

### Recombinant protein production

The selected variants and BsCotA encoding genes were codon-optimized for expression in *Escherichia coli* using DNAworks (Hoover and Lubkowski 2002) and were synthesized (Genscript, Nanjing, China). The synthetic genes were cloned into a pET24a vector (Novagen, Darmstadt, Germany) in fusion with the sequence for the C-terminal His-tag, using *Eco*RI and *Sal*I restriction sites. The copper-loaded laccase was produced following the protocol described in Durao et al. (2008). Briefly, *E. coli* strain BL21 (DE3) (Merck, Darmstadt, Germany) containing recombinant plasmids was grown overnight in 4 mL of Luria–Bertani medium supplemented with 50 µg/mL ampicillin, with shaking at 200 rpm. The cells were inoculated into 250 mL of Luria–Bertani medium and grown at 37 °C until $OD_{600}$ reached 0.6 ~ 0.8, moved to 16 °C, and supplemented with 0.25 mM $CuCl_2$ and 0.1 mM isopropyl-β-D-thiogalactopyranoside (IPTG). To produce the fully copper-loaded laccases, after 4 h of incubation, the shaker was switched off to achieve a microaerobic condition Durao et al. (2008). After further culture for 20 h, the cells were harvested by centrifugation at 8000 g for 20 min at 4 °C, and the resulting pellet was used for protein purification.

### Protein purification

The harvested cells were resuspended in the lysis buffer containing 50 mM Tris–HCl (pH 8.0), 100 mM NaCl, 1 mM $CuCl_2$, 1 mg/L of lysozyme, and 10 µg/L of benzonase. After 30-min incubation at ambient temperature, the cells were sonicated and the lysates were clarified by centrifugation at 8000 g for 20 min at 4 °C, and then loaded onto an immobilized metal affinity chromatography (IMAC) column (Bio-Rad, Hercules, CA, USA) equipped with a protein purification system (JP-blupadStar, Shanghai, China). The columns were washed with 50 mL lysis solution followed by 100 mL of lysis buffer with 35 mM imidazole. The bound BsCotA designs were eluted with 250 mM imidazole and analyzed by sodium dodecyl sulfate–polyacrylamide gel electrophoresis (SDS-PAGE) and ABTS oxidation activity. The eluted proteins were concentrated by ultrafiltration (Amicon Ultra, Sigma-Aldrich, St, Louis, MO, USA), and the imidazole was subsequently removed by dialysis at 4 °C overnight. The final enzyme concentration was determined by the Bradford assay (Lei et al. 2023).

### Enzyme activity assay

Enzyme activity assays were performed using ABTS as the substrate, in Britton-Robinson buffer at pH 4 and 70 °C.

Specifically, 3 µg/mL of the enzyme with 5 mM of ABTS was incubated with the enzyme for 5 min, and the reaction was quenched by adding an equal volume of methanol. The oxidation of ABTS was detected by measuring the absorbance at 420 nm using a spectrophotometer, with a molar extinction coefficient at 36 000 $M^{-1}$ $cm^{-1}$. All measurements were conducted in triplicates.

### Kinetics measurement

To determine the kinetics parameters of the purified laccase designs, enzyme assays were performed by reacting 1 µg/mL of the enzyme with varying concentrations of ABTS up to 2 mM at 70 °C for 5 min. The reactions were quenched after 5 min; the rates of oxidation were found to be linear during this time frame (Supplemental Fig. S1). The initial rates of ABTS oxidation were calculated from the amount of oxidized ABTS measured in each assay. All measurements were conducted in triplicates. The 2,6-dimerthoxybenzaldehyde (2,6-DMP) kinetic constants were measured at 70 °C and pH 6.0 for 5 min, and the reactions were quenched by adding of an equal volume of methanol. The oxidation of 2,6-DMP was detected by measuring the absorbance at 468 nm, with a molar extinction coefficient at 37,500 $M^{-1}$ $cm^{-1}$, while for guaiacol, the reactions were performed at 70 °C and pH 7.0 for 5 min, and the reactions were quenched by adding of an equal volume of methanol. The oxidation of guaiacol was detected by measuring the absorbance at 470 nm, with a molar extinction coefficient at 12,100 $M^{-1}$ $cm^{-1}$.

### Thermal stability

The thermal stability of BsCotA and its variants was evaluated by incubating aliquots across a broad temperature range, from 40 to 80 °C and pH 8.0 for 30 min. After incubation, these aliquots were diluted to Britton-Robinson buffer (pH 4.0) with 5 mM ABTS as the substrate, to measure the residual activity. The point at which a variant of BsCotA lost 50% of its original activity after incubation was denoted as $T_{50}$. Furthermore, kinetic thermostability along with $T_{50}$ was deduced by modeling the residual activity at variant temperatures to a 4-parameter Boltzmann sigmoidal curve:

$$At = A0 + \frac{A_f - A_0}{1 + e^{(T_{50} - T)/m}}$$

In the equation, $A_t$ represents the residual activity after incubating at a given temperature $T$; $A_0$ signifies the activity of the untreated control sample kept on ice, $A_f$ denotes the activity at the peak inactivation temperature, and $m$ stands for the sigmoidal slope coefficient. Additionally, these normalized rates were fitted to a 4-parameter Boltzmann sigmoid using the GraphPad Prism 7.0 (GraphPad Software, San Diego, CA). To ensure reliability, all measurements were executed in triplicate.

### Determination of optimum pH and pH stability

The optimum pH for the laccase reaction was determined by carrying out the reaction at 60 °C in Britton-Robinson (BR) buffers of varying pH values (1.0 to 7.0). The relative enzyme activity was determined by measuring the absorbance and the pH value with the highest activity was considered the optimum pH. Each experiment was repeated three times for accuracy.

The pH stability of the laccase was assessed by incubating the laccase in BR buffers with pH values ranging from 3.0 to 12.0 at 30 °C for 30 min, followed by measurement of the remaining enzyme activity under optimum conditions. Each experiment was repeated three times.

### Optimum temperature and temperature stability

The optimum temperature for the reaction was determined using the optimal pH previously determined. The enzyme activity was measured at temperatures ranging from 30 to 80 °C using spectrophotometry. The temperature with the highest enzyme activity was determined as the optimal reaction temperature. Each experiment was repeated three times for accuracy.

The temperature stability of CotA laccase was evaluated by incubating the enzyme at various temperature gradients from 45 to 85 °C for 30 min. The residual enzyme activity was then measured under optimal conditions. Each experiment was repeated three times for accuracy.

### Indigo carmine decolorization

The ability of the designed laccase to decolorize dye was evaluated by incubating 0.1 mg/mL indigo carmine in Britton-Robinson buffer with 0.1 mM ABTS as the mediator. Designed laccases were added at various concentrations up to 3.33 ng/mL. The reactions were carried out in 96-well plates at 30 °C with shaking for 12 h, with measurements taken every 10 min. The decolorization of indigo carmine was monitored by measuring the absorption at 602 nm.

## Results

### Design and generation of multi-point mutants

To enhance the ABTS oxidation efficiency of the laccase BsCotA, we utilized the FuncLib algorithm (Khersonsky et al. 2018) to detect potential mutations within the substrate binding grooves. The BsCotA binding site has been

precisely delineated via X-ray structural data 3ZDW (Bento et al. 2005) (Fig. 1). The two highly conserved histidines (His419, His497) and a single highly conserved cysteine, Cys492, which bond with copper ions, form the active site pocket of BsCotA (Fig. 1). The oxidized ABTS situates within a spacious pocket near His497. As the three highly conserved residues play vital roles in enzyme activities, they were omitted from our design process, in accordance with the FuncLib algorithm's directives (Khersonsky et al. 2018). We selected eight residues within the 4 Å range of ABTS (Fig. 1), specifically Pro226, Ala227, Thr260, Gly321, Gly323, Pro384, Leu386, and Gly417.

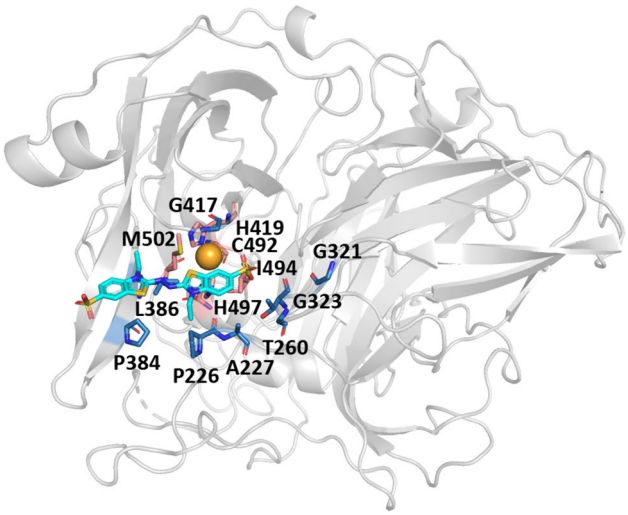


**Fig. 1** The active site pocket structure of BsCotA. The oxidized ABTS is shown in gray and located in the active site pocket. The BsCotA active site comprises a metal center (light orange sphere) of $Cu^{2+}$ ions that are liganded by two conserved histidine (deep salmon–colored sticks). The additional residues within the 4 Å range of ABTS comprise the active site pocket and are colored as blue sticks

The FuncLib initially reduced the search scope within those selected residues by implementing multiple sequence alignment, leading to the exclusion of infrequently occurring residues and those having a negative impact on protein folding energy, as determined by the Rosetta energy calculations (O'Meara et al. 2015). This effectively narrowed down the sequence searching scope from $8^{20}$ (approximately ~ $10^{13}$) to 456,663. Variants with fewer than two residues' differences were then grouped into a cluster, with the most stable variant having the lowest energy being chosen to represent each group. Ultimately, we achieved 50 designed variants, each having 3 ~ 5 mutation sites compared to the wild-type (Supplemental Table S1).

## Virtual screening of the designed variants

With an aim to lessen the experimental workload, we carried out a virtual screening of our specially 50 designed variants with the help of RosettaLigandDocking (DeLuca et al. 2015; Nguyen et al. 2013). As depicted in Supplemental Fig. S2, a significant proportion of the variants (45 out of 50) exhibited improved docking scores, hinting at their potential to provide enhanced activity against ABTS. Only 5 variants exhibited diminished scores. These findings indicate that our design methodology, rooted in the Funclib algorithm, was successful in spawning a diverse assortment of variants with a theoretical enhancement in activity. From the pool of 50 variants, we selected the highest-scored ones for ensuing experimental characterization. The F-09, F-20, F-26, F-28, and F-46 variants showed the highest affinity and were consequently chosen for additional analysis. Each of these variants contained 3 ~ 5 mutations and displays extensive variability in terms of mutated sites (Table 1).

**Table 1** Mutation sites and kinetic scores of wild-type BsCotA and five selected variants

| Laccases | Mutated site | Total score | Docking score | Specific activity (U/mg) | $K_M$ (mM) | $K_{cat}$ ($s^{-1}$) | $K_{cat}/K_M$ ($M^{-1}\,s^{-1}$) | $T_{50}$ |
|---|---|---|---|---|---|---|---|---|
| Wild-type | | −2162.71 | −10.71 | 128.90 | 0.79 ± 0.21 | 120.79 ± 4.78 | $1.54\times10^5$ | 67.55 ± 1.70 |
| F-09 | A227F/G321S/L386Y/G417F | −2108.38 | −14.57 | 225.27 | 0.23 ± 0.03 | 266.39 ± 11.31 | $1.18\times10^6$ | 72.53 ± 0.29 |
| F-20 | A227M/G321S/P384E/L386F/G417H | −2141.32 | −15.03 | 132.12 | 3.12 ± 0.89 | 342.11 ± 32.70 | $1.09\times10^5$ | 67.77 ± 1.73 |
| F-26 | A227S/G323N/P384E/L386F/G417H | −2074.56 | −14.77 | 134.39 | 1.43 ± 0.32 | 250.79 ± 39.18 | $1.76\times10^5$ | 68.60 ± 0.55 |
| F-28 | A227S/G321A/G323N/L386F/G417F | −2149.53 | −15.58 | 254.24 | 0.69 ± 0.13 | 424.13 ± 33.16 | $6.15\times10^5$ | 71.87 ± 0.31 |
| F-46 | A227Y/G321S/G323D/L386Y/G417H | −2119.37 | −15.22 | 196.68 | 0.19 ± 0.12 | 50.30 ± 8.49 | $2.59\times10^5$ | 57.64 ± 0.22 |

Note: Kinetic parameters were measured at pH 4 and 70 °C with ABTS as substrate

## Selected BsCotA variants exhibit improved catalytic activity

In order to contrast the properties of the wild-type and chosen BsCotA laccase variants, we purified them via Ni–NTA affinity chromatography. The purified CotA laccase demonstrated an approximately molecular weight of 65 kDa on SDS-PAGE (Supplemental Fig. S3), aligning with the reported molecular size of *B. subtilis* CotA laccase (Martins et al. 2002). Remarkably, all chosen variants displayed similar expression levels to the wild-type and revealed varying degrees of ABTS oxidation activity, suggesting that the variants retained functionality despite changes at the active site (Table 1). Four out of the five variants presented a minimum twofold enhancement in $k_{cat}$. F-46 is the sole variant to display a decreased $k_{cat}$, yet it exhibited improved affinity ($K_M$ of 0.19 mM) compared to the wild-type ($K_M$ of 0.79 mM). F-09 demonstrated a substantial reduction in $K_M$ from 0.79 to 0.23 mM, indicating a higher substrate affinity for ABTS compared to the wild-type. Although F-28 displayed unchanged $K_M$, it showed the highest $k_{cat}$ ($k_{cat}$ of 424 $s^{-1}$) among tested variants, around ~ 3.5-fold of the wild-type, and largely contributed to the catalytic efficiency (Fig. 2). Out of all the variants, the F-09 and F-28 performed well, enhancing their catalytic efficiency towards ABTS to $1.18 \times 10^6$ and $6.15 \times 10^5$ $M^{-1}$ $s^{-1}$ (Table 1), respectively. These values translate to 7.7-fold and 4.0-fold increases compared to the wild-type.

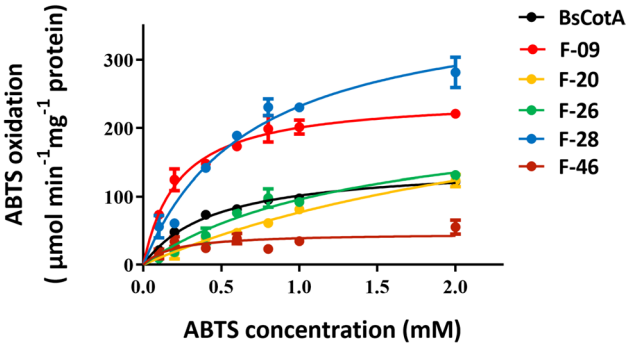


**Fig. 2** The kinetic parameters of BsCotA and selected variants. Data points represent the average of three independent measurements, and the error bars represent the standard deviation. The lines are the direct fit to Michaelis–Menten equation ($R.^2 \geq 0.97$). The resulting kinetic parameters are presented in Table 1

## Effects of temperature and pH on enzyme activity

To ascertain how the mutated residues of our most effective variants, F-09 and F-28, influence other biochemical properties, we measured the pH activity and stability profiles. The results indicated that both variants, as well as the wild-type BsCotA, displayed similar pH activity profile, with peak ABTS oxidation activity at pH 4.0 (Fig. 3A). The activity fell to less than 60% at pH values below 3. Moreover, BsCotA variants' activity diminished gradual as the pH level rose from 4.0 to 7.0. When the pH was increased to 7.0, both wild-type and the variants maintained approximately 30% of their activity, with no ABTS oxidation at the pH range of 8 ~ 12. In terms of pH stability, the wild-type laccase and F-09 and F-28 variants were incubated at different pH levels (from 3.0 to 12.0) at 30 °C for 30 min, and then assayed

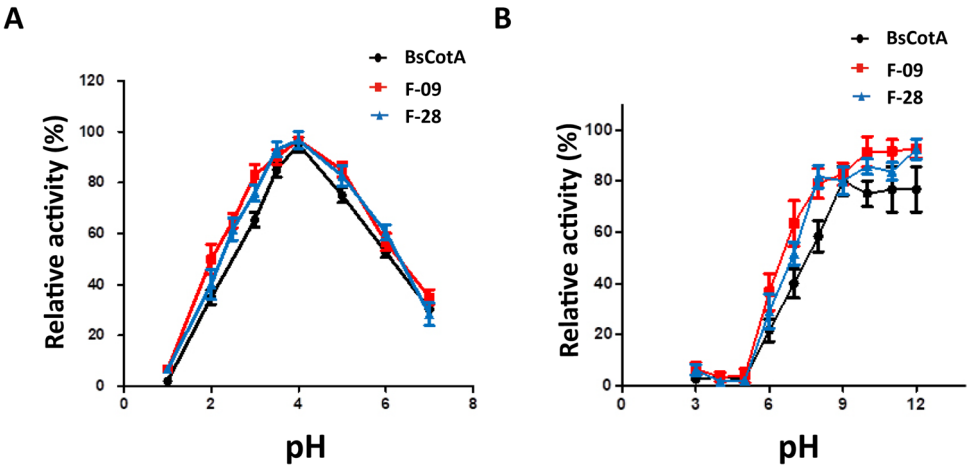


**Fig. 3** Optimal pH and pH stability of BsCotA variants. **A** Optimal pH of BsCotA variants. Black indicates wild-type CotA laccase, and red and blue indicate F-09 and F-28 variants, respectively. The dots represent the mean of relative activity, and the error bars represent standard deviation. Measurements were done in triplicate. **B** pH stability of BsCotA variants. Samples were incubated for different pH (3.0 ~ 12.0). The dots represent the mean of residual activity, and the error bars represent standard deviation. The X-axis represents different incubation pH values. Measurements were done in triplicate, and values obtained with the enzyme normalized to the enzyme incubated at pH 8

residual ABTS oxidation activity at pH 4. After half an hour incubation, a noticeable decrease in enzyme activity was apparent at acidic pH levels. However, the enzyme activity retained around 80% of its activity once the pH was raised to 9.0 (Fig. 3B).

Moving on, we analyzed the temperature activity profile and thermal stability of the laccase variants. These variants showed a comparable temperature activity pattern to the wild-type, functioning optimal activity at 70 °C and maintaining high activity within the 60 ~ 80 °C range (Fig. 4A). Moreover, both F-09 and F-28 variants exhibited similar thermal stability (Fig. 4B). The laccase variants were incubated at varying temperatures (ranging from 50 ~ 80 °C) for 30 min, and residual activity was measured at 70 °C. The wild-type BsCotA demonstrated an apparent $T_{50}$ of 67.55 °C. Slight improvement in $T_{50}$ was noted in the F-09 and F-28 design, with 72.53 °C and 71.87 °C, respectively. This complements the fact that our designs do not alter the enzyme's properties, particularly stability, compared to the wild-type.

## Catalytic efficiency of BsCotA laccase for different substrates

We also measured the catalytic efficiency of our variants with respect to other laccase substrates, including guaiacol and 2,6-DMP (Table 2, Supplemental Fig. S4 and S5). The catalytic efficiencies of all variants with 2,6-DMP declined to between 14 ~ 38% of that of the wild-type. In addition, substrate affinity. was also decreased, as indicated by a higher $K_M$. In contrast, F-09 demonstrated a slightly enhanced catalytic efficiency with guaiacol, at $1.79 \times 10^4$ $M^{-1}S^{-1}$, representing an improvement of approximately 70%. F-28 exhibited a level similar to the wild-type, while the other three variants showed varying degrees of reduced guaiacol turnover rate. These results

**Table 2** Kinetic constants of BsCotA' variants for ABTS, 2,6-DMP, and guaiacol oxidation

| Substrate | Variant | $K_M$ (mM) | $k_{cat}$ ($s^{-1}$) | $k_{cat}/K_M$ ($M^{-1}$ $s^{-1}$) |
|---|---|---|---|---|
| ABTS | Wild-type | 0.79 ± 0.21 | 120.79 ± 4.78 | $1.54 \times 10^5$ |
| | F-09 | 0. 23 ± 0.07 | 266.39 ± 11.31 | $1.18 \times 10^6$ |
| | F-20 | 3.12 ± 0.89 | 342.11 ± 32.70 | $1.09 \times 10^5$ |
| | F-26 | 1.43 ± 0.32 | 250.79 ± 39.18 | $1.76 \times 10^5$ |
| | F-28 | 0.69 ± 0.13 | 424.13 ± 33.16 | $6.15 \times 10^5$ |
| | F-46 | 0.19 ± 0.12 | 50.30 ± 8.49 | $2.59 \times 10^5$ |
| 2,6-DMP | Wild-type | 0.95 ± 0.09 | 10.81 ± 0.23 | $1.14 \times 10^4$ |
| | F-09 | 3.76 ± 0.53 | 14.47 ± 0.67 | $3.85 \times 10^3$ |
| | F-20 | 3.59 ± 0.54 | 5.79 ± 0.36 | $1.61 \times 10^3$ |
| | F-26 | 1.71 ± 0.25 | 6.09 ± 0.22 | $3.56 \times 10^3$ |
| | F-28 | 2.13 ± 0.37 | 9.30 ± 0.36 | $4.37 \times 10^3$ |
| | F-46 | 5.32 ± 0.85 | 8.92 ± 0.65 | $1.68 \times 10^3$ |
| Guaiacol | Wild-type | 0.65 ± 0.13 | 6.85 ± 0.19 | $1.05 \times 10^4$ |
| | F-09 | 0.31 ± 0.07 | 5.55 ± 0.08 | $1.79 \times 10^4$ |
| | F-20 | 2.15 ± 0.14 | 2.17 ± 0.14 | $1.01 \times 10^3$ |
| | F-26 | 1.54 ± 0.32 | 2.37 ± 0.14 | $1.54 \times 10^3$ |
| | F-28 | 0.52 ± 0.10 | 5.47 ± 0.19 | $1.05 \times 10^4$ |
| | F-46 | 0.96 ± 0.15 | 2.73 ± 0.10 | $2.84 \times 10^3$ |

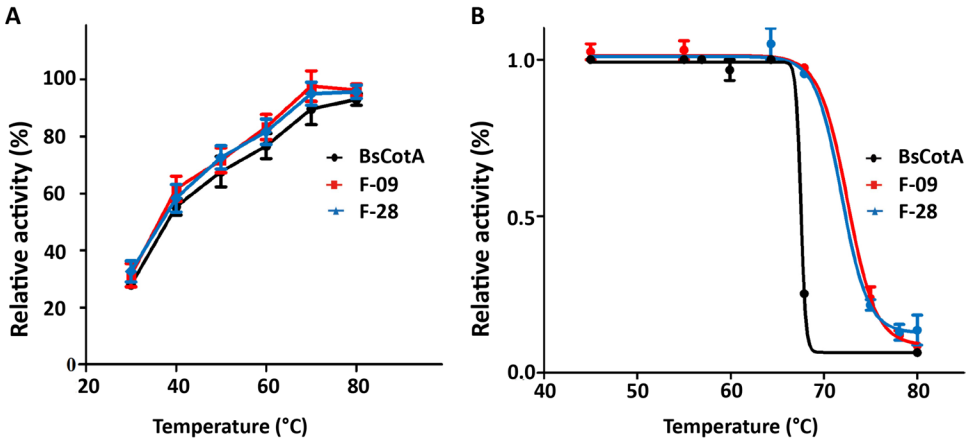


**Fig. 4** Optimum temperature and thermal stability of BsCotA variants. **A** Optimal temperature of CotA laccase (wild-type, F-09, and F-28). Black indicates WT (wild-type) CotA laccase, and red and blue indicate F-09 and F-28 designs, respectively. **B** The thermostability of BsCotA variants. The studied variants (WT, F-09, and F-28), were incubated at temperature of 50 ~ 80 °C for 30 min. Residual enzymatic activity was then measured with ABTS as substrate. Relative residual activity was derived from the initial rates of ABTS oxidation and plotted as a fraction of the activity of the enzyme incubated on ice. The dots represent the mean of residual activity, and the error bars represent standard deviation. The fit is based on a four-parameter sigmoidal curve ("Materials and methods"). Measurements were done in triplicate, and values obtained with the enzyme normalized to the enzyme incubated on ice

illustrate that the variants designed with different active sites have varying substrate biases.

## Indigo carmine dye decolorization

In order to evaluate the industrial applicability of our F-09 and F-28 variants, which demonstrated the highest ABTS oxidation activity, we conducted indigo carmine decolorization assays (Fig. 5 and Supplemental Fig. S6). The decolorization process involved using 0.1 mM ABTS as the mediator at pH 4 and 30 °C. Considering industrial applications, whether it is for lignin degradation or textile dye decolorization, the use of laccases ideally involves catalytic temperatures as close to room temperature as possible. Therefore, 30 °C was used for the decolorization reaction instead of the optimal temperature. As depicted in Fig. 5, both F-09 and F-28 variants showcased significant enhancements in decolorization across all inspected protein concentrations. At a protein concentration of 3 µg/mL, the wild-type BsCotA achieved complete decolorization within 1.8 h. Conversely, the F-09 variant accomplished comprehensive decolorization within merely 0.5 h, highlighting its superior efficacy. Additionally, F-09 and F-28 variants outperformed in decolorization at the lower protein concentration. The decolorization rate of the wild-type gradually dwindled with decreasing protein concentration, and it failed to achieve total decolorization at 1 µg/mL. However, the F-28 variant accomplished complete decolorization within 2.3 h at the same concentration, whereas the F-09 variant required only 1.8 h. Under identical conditions, the decolorization rate of the wild-type was only 69%, and reaching just 85% after a 12-h incubation period. Importantly, in the absence of BsCotA laccase, no decolorization was observed, serving as a negative control.

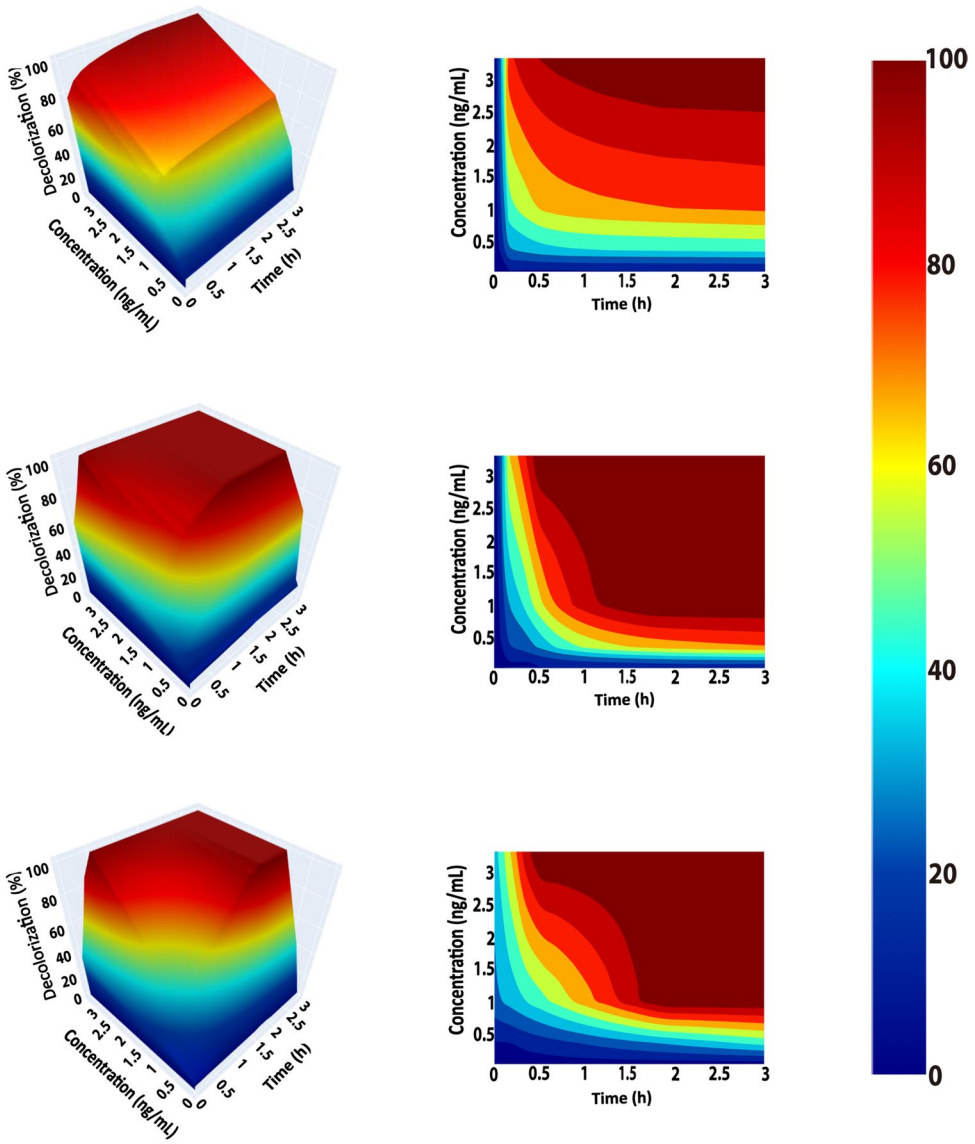


**Fig. 5** Indigo carmine decolorization within 2 h of incubation with BsCotA and variants (F-09 and F-28) shown with 3D surfaces and contour plots. The decolorization of indigo carmine (0.1 mg/mL) by wild-type, F-09, and F-28 variants was determined in 3 h of incubation using ABTS as a mediator at pH 4, the temperature of 30 °C

## Discussion

The performance of numerous laccase applications hinges significantly on the presence of mediators. This study aimed to enhance the catalytic efficiency of the heat-resistant laccase, BsCotA, for the prevalent mediator ABTS. The investigation designed variants with 3 ~ 5 mutated site using the Funclib algorithm, which has been credited for generating efficient and diverse enzyme (Khersonsky et al. 2018; Klaus et al. 2020). To reduce the screening labor cost, RosettaLigandDocking (DeLuca et al. 2015) was employed to screen the set of designed mutants. The top five variants with the highest docking scores were expressed and demonstrate improved $k_{cat}/K_M$ in subsequent experiments. These selected five variants showed comparable expression levels to the wild-type and varied levels of ABTS oxidation activity (Table 1). Findings imply that the Funclib algorithm influences only the interaction between the substrate and the active site pocket, not the catalytic residues, and does not cause a decrease in stability, a factor often observed in directed evolution methods (Goldsmith and Tawfik 2017). Four out of the five tested variants showed an increased turnover rate than the wild-type. Specifically, F-09 expressed the most considerable improvement, demonstrating a 7.7-fold increase in catalytic efficiency. On the other hand, the variant F-46 showed a decreased $k_{cat}$ and improved $K_M$, resulting in a 1.6-fold $k_{cat}/K_M$ of the wild-type.

To understand the molecular mechanism behind the difference in catalytic efficiency between our variants, a detailed structural analysis was carried out on the variants. All five selected variants with the highest docking scores had the mutation of Leu386 to an aromatic residue, either phenylalanine or tyrosine. This small-to-large substitution might decrease the active site pocket, optimizing the active site pocket geometry (Fig. 6), and limit the potential for movement within the active site pocket, thereby increasing $k_{cat}$. F-09 and F-28, the most efficient variants, displayed another significant mutation, G417F. The introduced benzene ring might cause a π-π stacking interaction with the benzothiazole ring of the ABTS molecule, assisting in substrate binding and subsequent electron transfer, thereby enhancing $k_{cat}$. Two similar mutations at the same positions, L386W and G417L, have been reported to amplify activity via laboratory evolution (Gupta et al. 2010). It is also noteworthy that F-46 displayed a decreased $K_M$ but lower turnover rates. The mutations G323D and G417H, which introduced charges into the hydrophobic pocket, may have disrupted favorable hydrophobic interactions, leading to an obvious decrease in $k_{cat}$.

Rational enzyme engineering prioritizes the manipulation of the active site residues to obtain enhanced enzyme catalytic efficiency. Oftentimes, achieving substantial improvements for specific substrates necessitates the introduction of multiple mutation sites. Computational tools have become indispensable for this task, helping to accelerate the optimization of biocatalyst (Scherer et al. 2021). FuncLib is a potent algorithm designed to introduce multipoint mutations within the activity pocket that consistently produce enzyme mutants with remarkably improved catalytical efficiency (Barber-Zucker et al. 2022; Khersonsky et al. 2018; Klaus et al. 2020; Risso et al. 2020). In this work, we employed ligand–protein docking simulations to screen a diverse set of BsCotA mutants designed using FuncLib. The top five BsCotA variants, as ranked by docking scores, were then analyzed. Notably, four variants expressed enhanced turnover rates, and the most promising variant evidenced a substantial 7.7-fold increase in $k_{cat}/K_M$.

The stability of our laccases warrants discussion. In our experiments, BsCotA and its variants exhibited reduced stability under the conditions of the kinetic assay with the substrate ABTS. Similar results have been reported in the literature (Wang et al. 2019). There are likely two main reasons for this phenomenon. Firstly, the absence of appropriate molecular chaperones during the heterologous expression in *E. coli* may have resulted in misfolding or partial non-native folding, leading to decreased stability. Secondly, although ABTS is widely used as a substrate for most laccase activity assays, the native function of BsCotA is the biosynthesis of the brown spore pigment (Martins et al. 2002). Therefore, it is plausible that BsCotA exhibits reduced stability under these non-native reaction conditions. Despite these factors, all variants were expressed, purified, and characterized under consistent conditions, and kinetic parameters were measured under conditions where the initial rates were linear (Supplemental Fig S1).

The results of indigo carmine decolorization are noteworthy. The reaction was carried with 0.1 mM ABTS as mediator. When 3.33 μg/mL protein was used, all tested BsCotA variants showed success to complete decolorization. Both F-09 and F-28 succeed in complete decolorization at even 1 μg/mL concentration, while the wild-type BsCotA failed completely decolorization at lower concentration. The better decolorization effect of two variants is supposed to get benefit from the improved $k_{cat}/K_M$, and reflected the better application potential, especially the F-09. Between the two tested variants, F-09 showed a faster decolorization at all tested applied protein concentration. F-09 and F-28 both variants displayed good decolorization capabilities, with F-09 showing a faster rate of achieving complete decolorization at nearly all tested concentrations. This could be attributed to F-09 having a lower $K_M$ compared to F-28, while the mediator ABTS concentration added to the reaction was only 0.1 mM. In this simulated application scenarios, both variants,

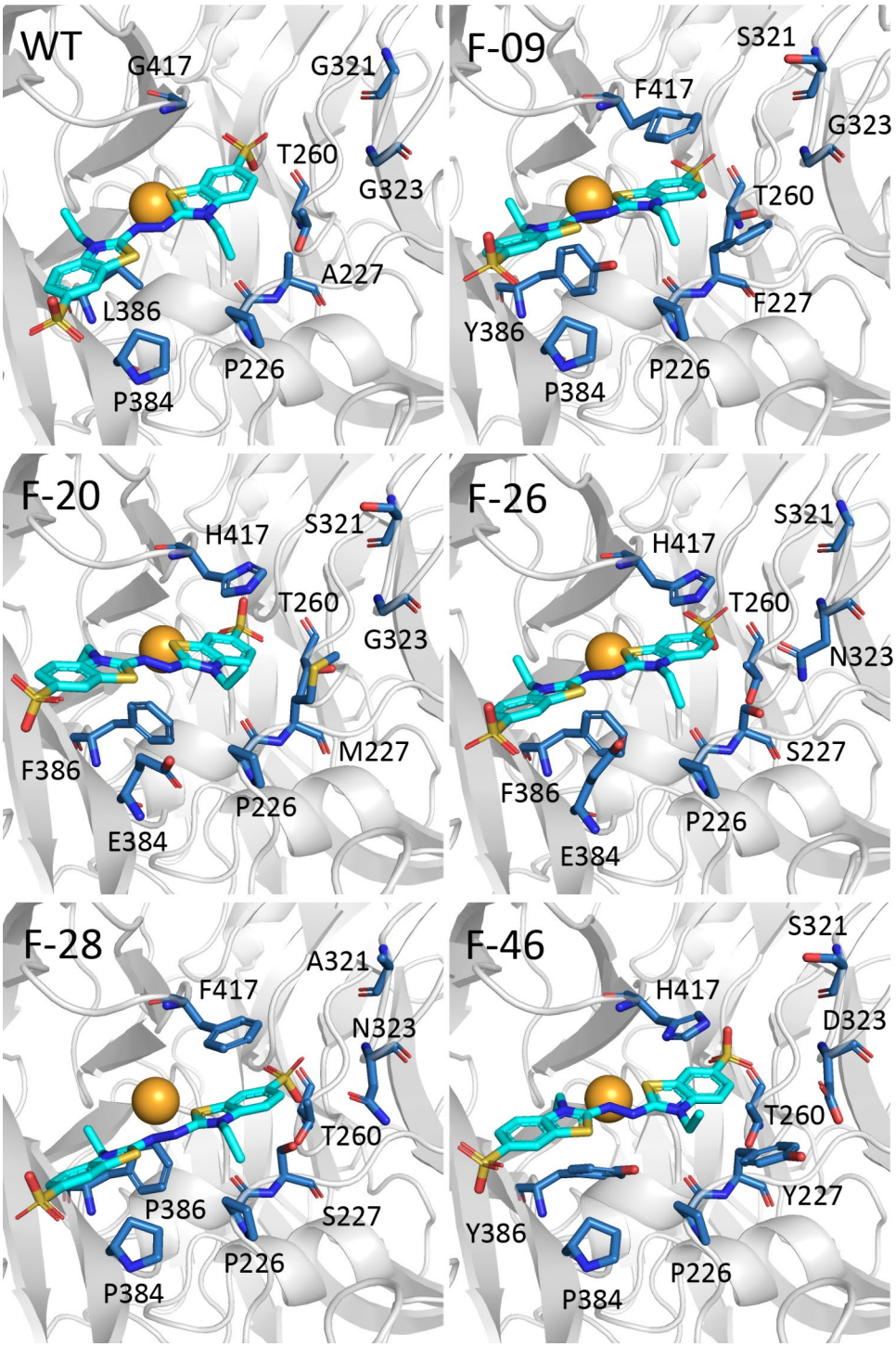


**Fig. 6** The stereochemical properties of the designed active site pocket of the BsCotA variants. The diagram shows the wild-type and its variants' active site pocket selected to present mutation of the amino acid, shown as a stick, with the spheres indicating the copper ions

especially F-09, demonstrated excellent potential for use. Another issue worth discussing in the dye decolorization assay is the apparent contradiction with the previous pH stability results of the enzymes. The three tested variants showed poor residual activity after incubation in acidic buffer (Supplemental Fig. S7). How, then, was an increase in decolorization observed after hours of incubation of BsCotA and its variants? In our assay, ABTS acted as the mediator and was initially oxidized the indigo carmine dye and subsequently returns to its reduced state. One possibility is that enough radical forms of ABTS accumulate before laccase inactivation, allowing these radicals to continue oxidizing the indigo carmine dye in subsequent reactions. Furthermore, despite the significant decrease in total enzymatic activity at acidic pH, sufficient residual activity might remain to facilitate the overall decolorization

process. Given enough time, this residual activity could drive the reaction efficiently. These combined factors can explain the observations in our experiments.

To enhance the catalytic efficiency of *B. subtilis* laccase BsCotA, towards the most commonly used mediator ABTS, we employed the Funclib algorithm for active site pocket design and combined with molecular docking for virtual screening to attempt. After that, extremely low throughout experimental screening is required. Five variants with top docking scores were characterized, and exhibited various levels of increase in $k_{cat}/K_M$, with the most significant enhancement being 7.7-fold, of which showed 2–4 folds enhancements, bringing $k_{cat}$ to the region of 200–400 $s^{-1}$. This value compares well with the best laccase reported to date, derived from extensive directed evolution efforts on complex rationally designed backgrounds (Mate et al. 2010; Mateljak et al. 2019). Finally, the $K_M$ of our best variant evolved from 0.79 to 0.23 mM, which is also a significant improvement. Admittedly, compared to successful modifications of laccase in other studies (Barber-Zucker et al. 2022; Mate et al. 2010), the F-09 from this study still has its limitations. However, the method used in this study, which does not require extensive experimental screening or multiple rounds of iteration, was able to achieve significant improvements in catalytic efficiency without negatively impacting the enzyme's thermal stability. To delve deeper into potential, our future research will focus on screening single and double mutants derived from our top variants, F-09 and F-28, and also attempting to combine mutation sites from these variants, such as introducing the G323N mutation from F-28 into F-09. This endeavor will not only aim to deepen our understanding of the molecular mechanisms governing the role of laccase's active site pocket residues in the substrate binding and catalysis but also to pave the way for further optimization strategies.

In summary, we successfully amplified the catalytic ability of laccase by using the FuncLib algorithm to design a set of variants and then performing virtual screening through protein–ligand docking. This brief workflow, which commenced with a very small-scale testing, resulted in a significantly improved design devoid of any loss in stability. Although this study focused on laccase, the computational approach presented here can also be applied to other enzymes. It may serve as a promising direction to develop more efficient biocatalysts.

**Supplementary Information** The online version contains supplementary material available at https://doi.org/10.1007/s00253-024-13291-3.

**Acknowledgements** We wish to thank the support from the State Key Laboratory of Biocatalysis and Enzyme Engineering.

**Author contribution** Y.H., L.Z., and C.Y. performed the experiment. J.Y. and L.L. supervised the study. Y.Z. and W. P. analyzed the data. L.L. designed and directed the project. Y.H. and L.L. wrote the manuscript with contributions from all authors. All authors contributed to the article and approved the submitted version.

**Funding** This work was supported by the National Natural Science Foundation of China (grant No. 31900089), Hubei Province key research and development program (grant No. 2021BCA113), and Opening Funding Project of the State Key Laboratory of Biocatalysis and Enzyme Engineering (grant No. SKLBEE2020021).

**Data availability** All data generated or analyzed during this study are included in this published article (and its supplementary information files).

## Declarations

**Human and animal rights** This article does not contain any studies with human participants or animals performed by any of the authors.

**Conflict of interest** The authors declare no competing interests.



## References

Barber-Zucker S, Mateljak I, Goldsmith M, Kupervaser M, Alcalde M, Fleishman SJ (2022) Designed high-redox potential laccases exhibit high functional diversity. ACS Catal 12(21):13164–13173. https://doi.org/10.1021/acscatal.2c03006

Bento I, Martins LO, Gato Lopes G, Armenia Carrondo M, Lindley PF (2005) Dioxygen reduction by multi-copper oxidases; a structural perspective. Dalton Trans 21:3507–13. https://doi.org/10.1039/b504806k

Camarero S, Martínez MJ, Martínez AT, García O, Vidal T, Colom J, del Río JC, Gutiérrez A (2002) Flax pulp bleaching and residual lignin modification by laccase-mediator systems. Prog Biotechnol 21:213–222

DeLuca S, Khar K, Meiler J (2015) Fully flexible docking of medium sized ligand libraries with RosettaLigand. PLoS ONE 10(7):e0132508. https://doi.org/10.1371/journal.pone.0132508

Durao P, Chen Z, Fernandes AT, Hildebrandt P, Murgida DH, Todorovic S, Pereira MM, Melo EP, Martins LO (2008) Copper incorporation into recombinant CotA laccase from *Bacillus subtilis*: characterization of fully copper loaded enzymes. J Biol Inorg Chem 13(2):183–193. https://doi.org/10.1007/s00775-007-0312-0

Enguita FJ, Marçal D, Martins LO, Grenha R, Henriques AO, Lindley PF, Carrondo MA (2004) Substrate and dioxygen binding to the endospore coat laccase from *Bacillus subtilis*. J Biol Chem 279(22):23472–23476. https://doi.org/10.1074/jbc.M314000200

Goldsmith M, Tawfik DS (2017) Enzyme engineering: reaching the maximal catalytic efficiency peak. Curr Opin Struct Biol 47:140–150. https://doi.org/10.1016/j.sbi.2017.09.002

Guo Y, Qin X, Tang Y, Ma Q, Zhang J, Zhao L (2020) CotA laccase, a novel aflatoxin oxidase from *Bacillus licheniformis*, transforms aflatoxin B1 to aflatoxin Q1 and epi-aflatoxin Q1. Food Chem 325:126877

Gupta N, Lee FS, Farinas ET (2010) Laboratory evolution of laccase for substrate specificity. J Mol Catal b: Enzym 62(3–4):230–234. https://doi.org/10.1016/j.molcatb.2009.10.012

Hakulinen N, Rouvinen J (2015) Three-dimensional structures of laccases. Cell Mol Life Sci 72(5):857–868. https://doi.org/10.1007/s00018-014-1827-5

Henriques AO, Moran CP Jr (2007) Structure, assembly, and function of the spore surface layers. Annu Rev Microbiol 61:555–588. https://doi.org/10.1146/annurev.micro.61.080706.093224

Hoover DM, Lubkowski J (2002) DNAWorks: an automated method for designing oligonucleotides for PCR-based gene synthesis. Nucleic Acids Res 30(10):e43. https://doi.org/10.1093/nar/30.10.e43

Ihssen J, Jankowska D, Ramsauer T, Reiss R, Luchsinger R, Wiesli L, Schubert M, Thony-Meyer L, Faccio G (2017) Engineered *Bacillus pumilus* laccase-like multi-copper oxidase for enhanced oxidation of the lignin model compound guaiacol. Protein Eng Des Sel 30(6):449–453. https://doi.org/10.1093/protein/gzx026

Khersonsky O, Lipsh R, Avizemer Z, Ashani Y, Goldsmith M, Leader H, Dym O, Rogotner S, Trudeau DL, Prilusky J, Amengual-Rigo P, Guallar V, Tawfik DS, Fleishman SJ (2018) Automated design of efficient and functionally diverse enzyme repertoires. Mol Cell 72(1):178-186 e5. https://doi.org/10.1016/j.molcel.2018.08.033

Klaus M, Buyachuihan L, Grininger M (2020) Ketosynthase domain constrains the design of polyketide synthases. ACS Chem Biol 15(9):2422–2432. https://doi.org/10.1021/acschembio.0c00405

Klobutcher LA, Ragkousi K, Setlow P (2006) The *Bacillus subtilis* spore coat provides "eat resistance" during phagocytic predation by the protozoan *Tetrahymena thermophila*. Proc Natl Acad Sci U S A 103(1):165–170. https://doi.org/10.1073/pnas.0507121102

Kothiwale S, Mendenhall JL, Meiler J (2015) BCL::Conf: small molecule conformational sampling using a knowledge based rotamer library. J Cheminform 7:47. https://doi.org/10.1186/s13321-015-0095-1

Lei L, Zhao L, Hou Y, Yue C, Liu P, Zheng Y, Peng W, Yang J (2023) An inferred ancestral CotA laccase with improved expression and kinetic efficiency. Int J Mol Sci 24(13). https://doi.org/10.3390/ijms241310901

Martins LO, Soares CM, Pereira MM, Teixeira M, Costa T, Jones GH, Henriques AO (2002) Molecular and biochemical characterization of a highly stable bacterial laccase that occurs as a structural component of the *Bacillus subtilis* endospore coat. J Biol Chem 277(21):18849–18859. https://doi.org/10.1074/jbc.M200827200

Mate DM, Alcalde M (2015) Laccase engineering: from rational design to directed evolution. Biotechnol Adv 33(1):25–40. https://doi.org/10.1016/j.biotechadv.2014.12.007

Mate DM, Alcalde M (2017) Laccase: a multi-purpose biocatalyst at the forefront of biotechnology. Microb Biotechnol 10(6):1457–1467. https://doi.org/10.1111/1751-7915.12422

Mate D, Garcia-Burgos C, Garcia-Ruiz E, Ballesteros AO, Camarero S, Alcalde M (2010) Laboratory evolution of high-redox potential laccases. Chem Biol 17(9):1030–1041. https://doi.org/10.1016/j.chembiol.2010.07.010

Mateljak I, Monza E, Lucas MF, Guallar V, Aleksejeva O, Ludwig R, Leech D, Shleev S, Alcalde M (2019) Increasing redox potential, redox mediator activity, and stability in a fungal laccase by computer-guided mutagenesis and directed evolution. ACS Catal 9(5):4561–4572. https://doi.org/10.1021/acscatal.9b00531

Morozova OV, Shumakovich GP, Gorbacheva MA, Shleev SV, Yaropolov AI (2007) "Blue" laccases. Biochem (moscow) 72(10):1136–1150. https://doi.org/10.1134/S0006297907100112

Nguyen E, Norn C, Frimurer T, Meiler J (2013) Assessment and challenges of ligand docking into comparative models of G-protein coupled receptors. PLoS ONE 8(7):e67302. https://doi.org/10.1371/journal.pone.0067302

O'Meara MJ, Leaver-Fay A, Tyka MD, Stein A, Houlihan K, DiMaio F, Bradley P, Kortemme T, Baker D, Snoeyink J, Kuhlman B (2015) Combined covalent-electrostatic model of hydrogen bonding improves structure prediction with Rosetta. J Chem Theory Comput 11(2):609–622. https://doi.org/10.1021/ct500864r

Reiss R, Ihssen J, Thöny-Meyer L (2011) *Bacillus pumilus* laccase: a heat stable enzyme with a wide substrate spectrum. BMC Biotechnol 11(1):9. https://doi.org/10.1186/1472-6750-11-9

Risso VA, Romero-Rivera A, Gutierrez-Rus LI, Ortega-Muñoz M, Santoyo-Gonzalez F, Gavira JA, Sanchez-Ruiz JM, Kamerlin SCL (2020) Enhancing a de novo enzyme activity by computationally-focused ultra-low-throughput screening. Chem Sci 11(24):6134–6148. https://doi.org/10.1039/D0SC01935F

Riva S (2006) Laccases: blue enzymes for green chemistry. Trends Biotechnol 24(5):219–226. https://doi.org/10.1016/j.tibtech.2006.03.006

Scherer M, Fleishman SJ, Jones PR, Dandekar T, Bencurova E (2021) Computational enzyme engineering pipelines for optimized production of renewable chemicals. Front Bioeng Biotechnol 9:673005. https://doi.org/10.3389/fbioe.2021.673005

Shankar S, Shikha (2014) Effect of metal ions and redox mediators on decolorization of synthetic dyes by crude laccase from a novel white rot fungus *Peniophora* sp. (NFCCI-2131). Appl biochem biotechnol 175. https://doi.org/10.1007/s12010-014-1279-2

Vetting MW, Al-Obaidi N, Zhao S, San Francisco B, Kim J, Wichelecki DJ, Bouvier JT, Solbiati JO, Vu H, Zhang X, Rodionov DA, Love JD, Hillerich BS, Seidel RD, Quinn RJ, Osterman AL, Cronan JE, Jacobson MP, Gerlt JA, Almo SC (2015) Experimental strategies for functional annotation and metabolism discovery: targeted screening of solute binding proteins and unbiased panning of metabolomes. Biochem 54(3):909–931. https://doi.org/10.1021/bi501388y

Wang X, Bai Y, Huang H, Tu T, Wang Y, Wang Y, Luo H, Yao B, Su X (2019) Degradation of aflatoxin B1 and zearalenone by bacterial and fungal laccases in presence of structurally defined chemicals and complex natural mediators. Toxins 11(10):609